Available online at www.sciencedirect.com
SCIENCE DIRECT®
Journal of Solid State Chemistry 172 (2003) 471–479
JOURNAL OF SOLID STATE CHEMISTRY
http://elsevier.com/locate/jssc

Structural and thermal study of calcium undecanoate

A. Valor,[a,b,*] S. Kycia,[c] E. Torres-García,[d] E. Reguera,[a] C. Vázquez-Ramos,[e] and F. Sánchez-Sinencio[f]

[a] *Facultad de Física, IMRE, Universidad de La Habana, San Lázaro y L, Vedado, La Habana 10400, Cuba*
[b] *Centro de Investigación en Ciencia Aplicada y Tecnología Avanzada-IPN, Legaria 694, Col. Irrigación, México D.F. 11500, Mexico*
[c] *Laboratório Nacional de Luz Síncrotron, Caixa Postal 6192, CEP 13084-971, Campinas, S.P., Brazil*
[d] *Instituto Mexicano del Petróleo, Eje Central Lázaro Cárdenas 152, México D.F. 07730, Mexico*
[e] *Instituto de Investigaciones en Materiales, UNAM, AP 70-360. México D.F., Mexico*
[f] *Departmento de Física, CINVESTAV-IPN, AP 14-740, México D.F. 07360, Mexico*

Received 27 September 2002; received in revised form 11 December 2002; accepted 15 December 2002

Abstract

In the present work, an X-ray diffraction (XRD) and thermal study of calcium undecanoate is presented. The measured high-resolution XRD powder pattern of the synthesized salt at room temperature, using synchrotron radiation, showed that the salt is a mixture of monohydrated and anhydrous calcium undecanoate. Calcium undecanoate monohydrate proved to have a monoclinic cell with a symmetry described by the $P2_1/a$ space group. The structure dehydrates at about 100°C. After dehydration, the salt undergoes a phase transformation which results in a thermotropic mesophase. Further heating of the salt leads to decomposition and melting. Ketones are the probable products of decomposition at 400°C.

Keywords: Calcium undecanoate; Powder diffraction; Thermal analysis; Infrared spectroscopy; Thermal decomposition; Synchrotron radiation

1. Introduction

Calcium soaps are materials that serve a wide range of industrial applications as detergents, softeners, plasticizers, greases, lubricants, cosmetics and medicines. Their selection for specific applications is governed by their fundamental properties [1].

Calcium salts of unsaturated carboxylic acids are also of interest because of their presence in the staple food of Mexican and other Central American peoples: the corn tortilla [2].

However, many metal soaps have been poorly characterized and most studies have been carried out several decades ago using XRD and thermal methods available at that time.

Because of their wide use in industry, the knowledge of the structural and thermal behavior of the alkaline metal soaps is of interest.

The present work is part of a more ambitious systematic study of the calcium salts of aliphatic carboxylic acids with different chain lengths [3–5]. It deals with studies of infrared, X-ray, differential scanning calorimetry (DSC) and thermogravimetric analysis (TGA) of calcium undecanoate carried out in order to investigate the structure and thermal behavior of this calcium salt in the solid state.

2. Experimental

The calcium salt of undecanoic acid was prepared from SIGMA grade $Ca(OH)_2$ and undecanoic acid (CH_3–$(CH_2)_9$–CO_2H), using the same procedure previously described [5]. We will call the obtained sample C_{11}.

The XRD powder patterns were measured in a Siemens D5000 diffractometer using CuKα radiation at 40 kV and 30 mA, with a diffracted beam graphite monochromator. The measurements were performed at room temperature in the 2–50°–2θ range, measuring 20 s

*Corresponding author. Departmento de Física, CINVESTAV-IPN, Ave. Instituto Politécnico Nacional No. 2508, AP 14-740, México D.F. 07360, Mexico. Fax: +52-5747-3832.
E-mail address: almavalor@yahoo.com (A. Valor).

0022-4596/03/$ - see front matter © 2003 Elsevier Science (USA). All rights reserved.
doi:10.1016/S0022-4596(03)00042-2

per point every 0.01°–2θ. An external silicon standard was used for 2θ calibration.

Also, powder diffraction measurements were performed using synchrotron radiation at the XRD1 beam line of the National Synchrotron Light Laboratory (LNLS) in Campinas, Brazil.

The registries were carried out at energies around 7 keV ($\lambda = 1.7611$ and 1.7620 Å), obtained with a double Si(111) sagittal monochromator. The wavelength calibration was made by measuring the powder diffraction pattern of an Al_2O_3 NIST standard. The full-width at half-maxima (FWHM) of the peaks were on average 0.05° 2θ. This pattern was indexed with figures of merit [6,7] $M_{20} = 450$ and $F_{30} = 700$.

For all measurements, the diffractometer chamber was evacuated and then filled with helium to minimize the absorption of the X-rays. The patterns of the studied sample were measured between 1 and 65° 2θ with a step of 0.01° 2θ. The incident beam intensity was monitored by means of an ionization chamber. The diffracted intensity was normalized in the course of the measurement. Several scans were made until the obtained signal-to-noise ratio was satisfactory.

The temperature-dependant powder diffraction patterns were measured at LNLS under the same conditions, with the addition of a high-temperature furnace, mounted at the center of the diffractometer. The furnace temperature was computer controlled with a 0.5°C precision.

For all measurements (in a conventional diffractometer or at the LNLS beam line), the samples were ground in an agate mortar and carefully loaded in a rotating flat plate specimen holder without applying too much pressure, in order to minimize the preferential orientation of the crystallites.

The diffraction peak positions and relative intensities were determined making use of the WinFit [8] program with asymmetric Pearson functions. The zero point of the XRD patterns was evaluated through the harmonics method.

Patterns were indexed using the powder indexing system CRYSFIRE [9]. Then, the best cell solution and the space group were evaluated with the cell-refining program CHECKCELL [10].

The infrared (IR) spectra at room temperature were measured by means of a Brucker Equinox 55 Fourier Transform Infrared (FTIR) spectrometer. The specimens were prepared in KBr pressed disks.

Temperature dependant IR spectra were taken in a Brucker IFS 66 spectrometer with a temperature controlled cell constructed for the purpose. The cell had calcium fluoride windows, with absorption bands below 1000 cm^{-1}. During the measurements, a dry air flow was circulated through the cell at 40 mL/min. In this case, the samples were also prepared in KBr disks.

The thermogravimetric analysis (TGA) measurements were carried out using a high-resolution thermobalance (TGA Hi-Res, TA Instrument, TG-2950 Model) using N_2 flow of 100 mL/min. The programmed heating rates were 5, 10, 20 and 50°C/min with an instrumental resolution of 5. The sample weight was approximately 12 mg in all cases. The Hi-Res TGA technique allowed a predefined temperature program to be followed in ranges where there was no modifications in the solid, it was possible to have a high heating rate, but when a mass loss was detected the heating rate was reduced towards zero, and kept low until the mass again became nearly constant [11].

The data of modulated differential scanning calorimetry (MDSC) (TA Instruments MDSC-2950 Model) were obtained under the following conditions: stabilized initial temperature of 25°C for 5 min, modulation of $\pm$0.318°C each 60 s, with a ramp of 2°C/min until 360°C in a N_2 atmosphere and hermetic pans. In MDSC, the same heat flux arrangement as in the DSC cell was used, but a different temperature (heating/cooling) profile was applied to the sample and reference via the furnace. Specifically, a sinusoidal modulation was overlaid on the standard linear temperature ramp. As a result, there were three heating-related experimental variables: heating rate, amplitude of modulation, and modulation frequency, which could be used to improve DSC results. MDSC determines the total, as well as the individual heat flow components (reversible and nonreversible heat flows) and provides an increased understanding of complex transitions in materials [12].

3. Results and discussion

The absence of the reagents in the obtained sample was checked by means of IR spectroscopy. Fig. 1 shows the IR spectra at room temperature of $Ca(OH)_2$, undecanoic acid and the synthesized salt.

The main absorption band that identifies the $Ca(OH)_2$ corresponds to the stretching vibrations of the O–H group at 3643 cm^{-1}. In the undecanoic acid spectrum the strong C=O stretching band can be seen in the region 1715–1708 cm^{-1}, which is characteristic of the carboxylic acids.

The complete disappearance of the strong absorption band near 1700 cm^{-1} in the spectrum of the C_{11} sample indicates that there is a complete resonance between the two carbonyl bonds of the carboxylic group of the salt molecule and the two C–O bonds such that they become identical in their force constant, assuming an intermediate value between those normal double and single bonds. The appearance of two absorption bands of the carboxyl group corresponding to symmetric and asymmetric stretching vibrations of the carboxylate ion near 1410 and 1530 cm^{-1} in this spectrum, instead of one

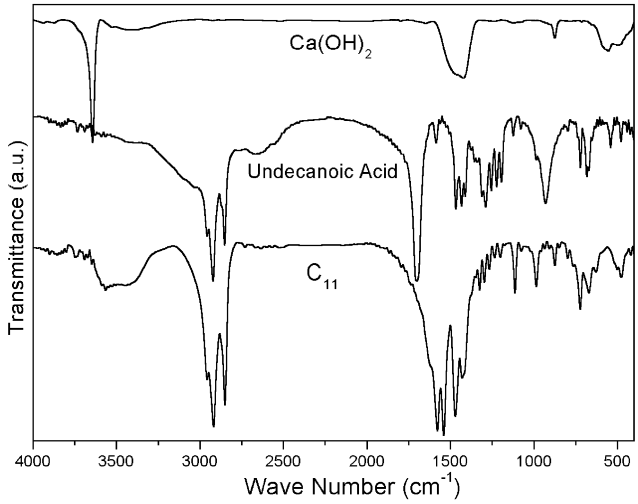

Fig. 1. Comparison between IR spectra for $Ca(OH)_2$, undecanoic acid, and the synthesized sample C_{11}.

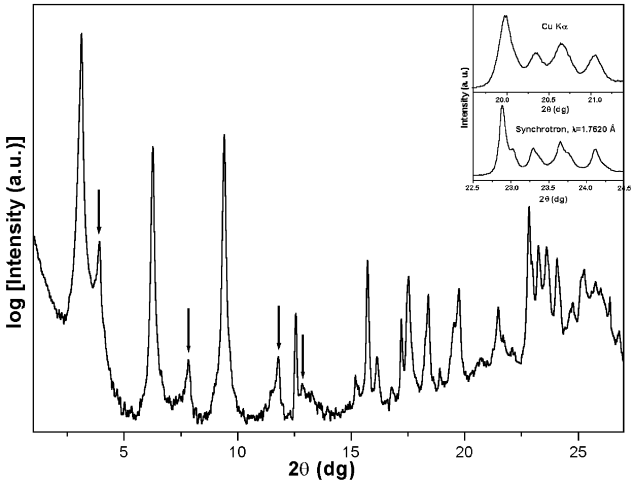

Fig. 2. XRD pattern of C_{11} measured using synchrotron radiation ($\lambda = 1.7620$ Å). The arrows indicate the reflections that were excluded from the pattern indexing. In the inset: a comparison of a section of the pattern measured with CuKα and synchrotron radiation.

band near 1700 cm^{-1}, confirms that the obtained sample C_{11} is a salt that possesses an ionized structure and that the metal–oxygen bonds in the soap have an ionic character. On the other hand, the sharp strong band corresponding to stretching vibrations of the O–H group at 3643 cm^{-1} has disappeared. One more detail observed in the IR spectrum of the salt is the presence of a broad absorption band in the region 3700–3200 cm^{-1} and a weak band at about 1620 cm^{-1}. These bands can be assigned to the stretching vibrations and to bending of water of crystallization, respectively; indicating the presence of water in this compound. The assigned frequencies are in good agreement with the results of other authors [13].

From the weight loss that was observed at about 100°C in the TGA curve (Fig. 5), corresponding to the loss of 1 mole of water per mole of calcium undecanoate, it was established that the sample is a monohydrate $[(CH_3–(CH_2)_9–CO_2)_2Ca:H_2O]$. It is reasonable to assume that the water molecule is coordinated to the calcium atom in the salt.

3.1. Room temperature XRD of the sample C_{11}

When the XRD powder pattern was measured in a conventional diffractometer it was not possible to index the pattern because of the strong overlapping of the reflections in the region of $q = 1.4-1.6$ Å^{-1} ($q = (4\pi/\lambda)\sin\theta$, $2\theta = 19.8-22.6°$). In the insert of Fig. 2 a comparison of a section of the measured patterns using CuKα and synchrotron radiation, respectively is shown. Several diffraction peaks could only be resolved by measuring the pattern at a synchrotron source because of its parallel beam and high-resolution diffractometer geometry.

The diffraction pattern of the synthesized sample C_{11} (Fig. 2) shows the main characteristics found in the patterns of calcium salts of aliphatic carboxylic acids [3]:

(i) At low diffraction angles a series of intense, very sharp (FWHM = 0.05° 2θ) and equidistant peaks appear. These peaks must correspond to long range ordering of planes whose interplanar distances d are large. These reflections define the long axis of the cell, which should be a multiple of the length of the units conforming the aliphatic chain [14]. The fact that the reflections belonging to this group are equidistant indicates that they correspond to different orders of the same family of planes.

(ii) In higher 2θ positions, groups of reflections that must correspond to smaller d spacings and much smaller parameters of the unit cell are observed [14].

(iii) Some of these high angle reflections show a considerable peak broadening (Fig. 2). This can be indicative of disorder in the crystalline network of planes that do not contain calcium atoms and that are related to the aliphatic chain.

Exceptions to the previously mentioned general trend are the low intensity peaks that are marked with arrows in Fig. 2. The first three peaks, are also equidistant to each other and it could be that they are satellite peaks of the reflections corresponding to long range periodic order.

This breaking of the regularities in the C_{11} diffraction pattern might be an indication of the presence of a second phase, with a crystalline cell smaller than the one of the corresponding hydrate in study. The presence of this second phase was corroborated, as it will soon be

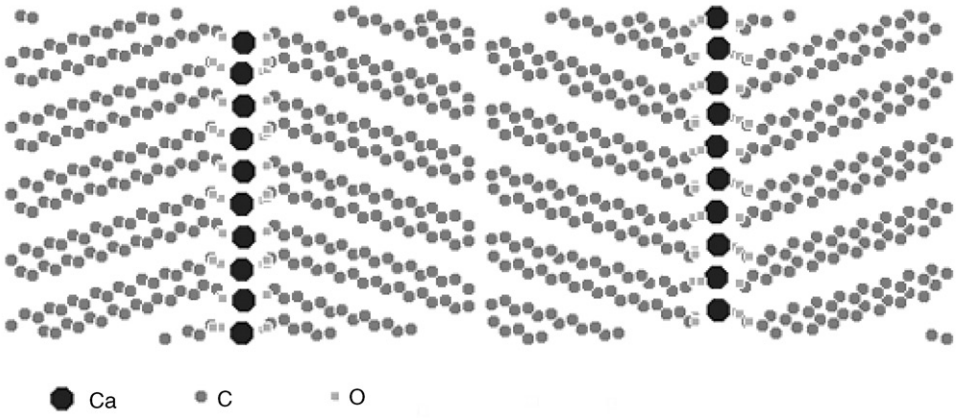

Fig. 3. Schematic crystalline structure of an aliphatic calcium carboxylate monohydrate. After [15].

seen, with the thermal studies and turned out to be the corresponding anhydrous salt.

With the assumption that these small peaks belong to a second phase, they were excluded from the list of reflections used to index the pattern. Twenty reflections were used for indexing and refining the cell. As a result, a monoclinic cell with cell parameters: $a = 64.4473$ (31) Å, $b = 6.8067$ (4) Å, $c = 5.8892$ (2) Å, $\beta = 90.70$ (0)° was obtained. The de Wolff's [6] and Snyder's [7] figures of merit $M_{20} = 45.1$ and $F_{20} = 150$, together with the calculated density ($D_m = 1.102\,g/cm^3$; $Z = 4$) which is common for such a compound, show that this cell is both mathematically and physically correct. In addition, the observed linear dependence of value of the cell parameter a, on the number of carbon atoms in the aliphatic chain, reported previously [4], is another indication of the correctness of this result. This dependence is indicative of the stacked layer character of the crystalline structure, which has been schematically represented in Fig. 3 after Lelann and Bérar [15]. These authors have solved the structure for calcium stearate monohydrate and their result could be the starting point for refining the crystalline structure of calcium undecanoate monohydrate.

In Table 1 the diffraction data for calcium undecanoate monohydrate are given. From the observed extinction conditions (h even for the ($h0l$) and ($h00$) reflections and k even in ($0k0$) reflections) it could be established that the indexed XRD pattern is consistent with the $P2_1/a$ space group. This is in agreement which the space group assigned to other calcium monohydrates of aliphatic carboxylic acids [4,15].

Table 1
Powder diffraction data for calcium undecanoate monohydrate

h	k	l	$2\theta_{obs}$ (°)	$2\theta_{calc}$ (°)	d_{obs} (Å)	I/I_0
−2	0	0	3.125	3.134	32.3097	100
−4	0	0	6.266	6.269	16.1196	38
−6	0	0	9.414	9.410	10.7360	69
−8	0	0	12.558	12.558	8.0552	3
−10	0	0	15.719	15.715	6.4427	8
−4	1	0	16.151	16.155	6.2715	2
0	0	1	17.207	17.208	5.8892	4
2	0	1	17.525	17.533	5.7832	9
4	0	1	18.400	18.404	5.5103	6
−6	0	1	19.544	19.545	5.1907	4
6	0	1	19.749	19.749	5.1373	7
8	0	1	21.491	21.485	4.7252	5
−10	1	0	21.696	21.703	4.6811	3
−1	1	1	22.859	22.860	4.4459	23
−2	1	1	23.014	23.010	4.4163	13
−3	1	1	23.278	23.268	4.3669	13
−4	1	1	23.633	23.631	4.3022	16
4	1	1	23.745	23.744	4.2822	12
−5	1	1	24.089	24.093	4.2220	13
−6	1	1	24.650	24.650	4.1273	5

Average difference between observed ($2\theta_{obs}$) and calculated ($2\theta_{calc}$) values is 0.01°.
Synchrotron radiation ($\lambda = 1.7620$ Å). Monoclinic system. Space group: $P2_1/a$. $Z = 4$. $a = (64.4473 \pm 0.0031)$ Å, $b = (6.8067 \pm .0004)$ Å, $c = (5.8892 \pm .0002)$ Å, $\alpha = 90°$, $\beta = (90.700 \pm 0.001)°$, $\gamma = 90°$, $V = 2583.270$ Å^3.

3.2. Thermal study of C_{11}

The thermal profile of the synthesized sample, obtained by MDSC in the range from room temperature to 360°C is presented in Fig. 4. The total, reversible, and nonreversible heat flows are included. Five thermal events, that have been marked with Roman numbers in the figure, can be distinguished.

The endothermic effect (I), at around 120°C, is essentially nonreversible. It is associated to the dehydration of the solid. The reversible portion of the heat at this temperature is related to a possible rehydration of a fraction of the material due to the elevated partial water pressure, resulting from the use of a closed crucible.

Fig. 5 shows the Hi-Res TGA curves of the same sample, measured at different heating rates, in the temperature range where the dehydration takes place. The weight loss associated to this process is equivalent

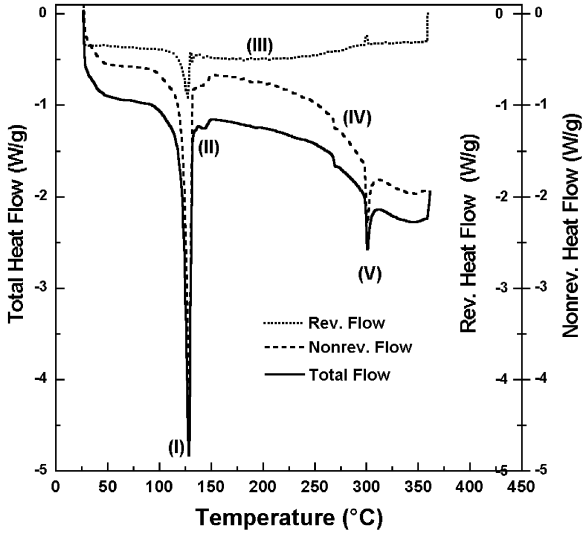

Fig. 4. Modulated DSC curves of C_{11}. The main processes are indicated with Roman numbers.

to 3.9% of the initial mass. This would give a slightly inferior mass loss than the corresponding to a water molecule per molecule of the solid. This difference is attributed to the presence of a second anhydrous phase in the synthesized sample.

The small endothermic process (II), contiguous to dehydration, at 135°C must correspond to a phase transition in the anhydrous salt. Previously, two endothermic peaks in the DSC diagram of calcium propionate monohydrate for temperatures around 120°C were also observed [16]. The first peak was assigned to dehydration, but the origin of the second endothermic peak was not explained. They just correlated its occurrence with the sample mass. Judging by the experiment presented in that work, according to which the second endothermic peak gets more pronounced, in comparison with the first one, as the hydration degree of the salt diminishes, until it becomes practically unique for the anhydrous salt, it can be concluded that it corresponds to a phase transformation of the anhydrous salt.

It has to be noticed that in the Hi-Res TGA curves (Fig. 5) no process corresponding to the DSC event (II) was observed, eliminating, therefore, the possibility of the existence of a second hydrated phase that dehydrates at higher temperature than the monohydrate.

Thermal event (III), present in the reversible heat curve obtained by MDSC (Fig. 4), has been related to the superficial water adsorption by the solid. The heat related to it, is interpreted like the heat necessary to desorb the superficial water. The reversible heat of these three first processes can be possibly detected only when a considerable partial water pressure exists at the immediate vicinity of the place where the dehydration reaction occurs. The intermediate metastable hydrate formation by recombination has been widely discussed in Ref. [17]. It has been shown that the partial pressure of the gas product of the reaction, the heating rate and the size and morphology of the particles are important aspects to consider in a dehydration reaction. They are decisive elements for a well sustained and coherent analysis.

The degradation stage of calcium undecanoate can be located from 160°C with successive mass losses (see Fig. 6). The decomposition of the salt takes place in a gradual and continuous form, as it can be seen from the weight loss in the figure, unlike calcium propionate, where the formation of intermediates was reported [18].

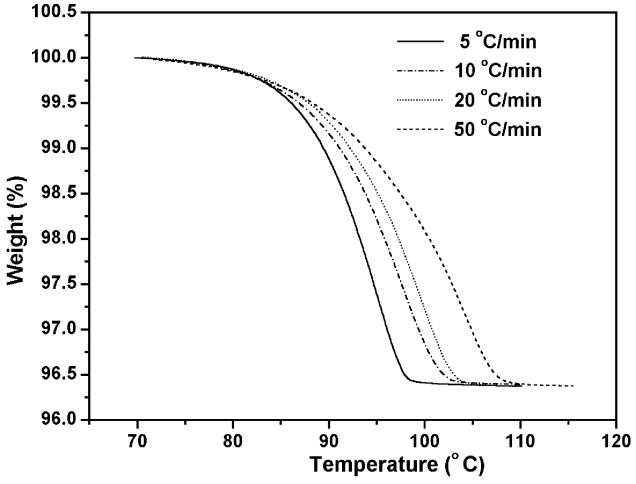

Fig. 5. High-resolution TGA curves of C_{11} for four different heat rates. The mass loss is equivalent to 3.9% of the initial mass.

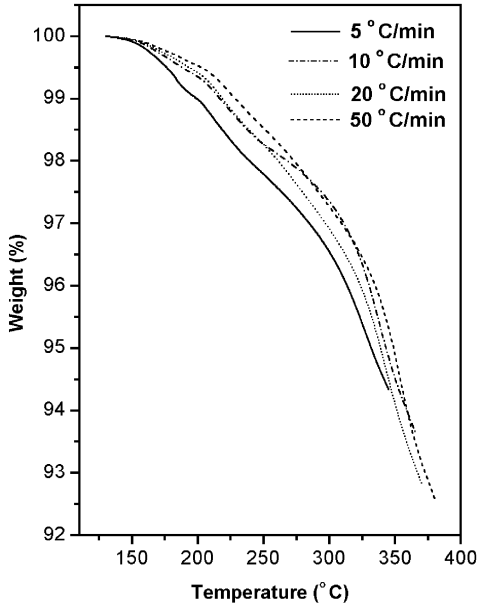

Fig. 6. High-resolution TGA curves of C_{11} for the decomposition process obtained at several heating rates: 5°C, 10°C, 20°C and 50°C/min.

The two first processes observed in the Hi-Res TGA curves in Fig. 6 correspond to losses of 0.75% and 2% of the mass of the anhydrous sample (after dehydration), respectively. These percent values are equivalent to 3.1 and 8.2 u, respectively. That is to say, they can only be associated to the release of hydrogen atoms ($m_H = 1.008$ u) from the chain. The certainty that these processes are related to changes in the aliphatic chain will be established soon by means of infrared spectroscopy with temperature.

The liberation of hydrogen during the decomposition of an aliphatic calcium salt has been suggested by O'Connell and Dollimore [18], who pointed to $CaCO_3$, CH_4 and CO like the most probable products of calcium propionate decomposition. If we take this statement as valid it is reasonable to conclude that to maintain a charge balance the liberation of two hydrogen atoms per C–C bond is necessary.

The most important thermal events observed by MDSC that can be related to decomposition take place at temperatures over 250°C (Fig. 4). The slope change in the baseline of the DSC curve (event IV) is related to the beginning of processes, like bonds breaking.

The reversible endothermic effect at 300°C (event V), is determined by the occurrence of the fusion of the sample and probably takes place simultaneously with the decomposition of a part of the solid, initiated from inferior temperatures [19]. This can justify that the portion of the reversible heat is not proportional to the heat flow initially involved. The value of the melting temperature agrees with the criteria about the occurrence of melting process for the aliphatic calcium salts at temperatures over 200°C [20].

3.3. X-ray diffraction with temperature

With the objective to abound in the structural changes involved in the dehydration process of calcium undecanoate monohydrate, the evolution of the XRD patterns with temperature was followed.

In Fig. 7, the diffraction patterns measured using synchrotron radiation at three different temperatures are presented. At room temperature, as it had been previously noticed, the main phase: calcium undecanoate monohydrate, together with a second phase (indicated with arrows) are present. As the temperature increases (see the pattern obtained at $T = 85$°C) the peaks of this second phase are moved towards smaller angles, indicating the expansion of the crystalline cell. For a temperature above the dehydration temperature ($T = 110$°C) the reflections of the monohydrate, like it could be expected, have disappeared.

It can be seen that the peaks of the residual phase that was present in the synthesized sample, are those which have increased their intensity at expenses of the monohydrated phase. This fact confirms that this is an anhydrous calcium undecanoate phase.

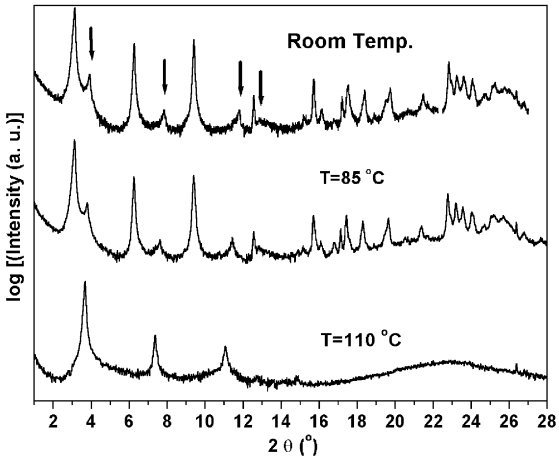

Fig. 7. XRD patterns of C_{11} measured in a temperature furnace using synchrotron radiation ($\lambda = 1.7611$ Å).

It should be pointed out that the peaks that were marked with arrows and that belong to the diffraction pattern of the anhydrous salt, at 110°C are sharp reflections that must correspond to the planes (h00) (with even h), whereas the reflections corresponding to small interplanar distances are so wide and low intense that they cannot be solved, indicating to the loss of crystallinity of the corresponding planes. This means that in the phase obtained after dehydration there are very well-defined crystalline planes parallel to the basal plane (b, c), whereas the rest of the planes have lost its crystalline order.

In other words, the structure of the anhydrous phase can be described like the one of a liquid crystal, that is to say, a phase that is crystalline in the direction of the long range axes, because the reflections corresponding to these planes are intense and sharp, and amorphous or liquid laterally since the peaks that correspond to short distances are diffuse.

This confirms the assignation done to the endothermic peak (II) in the MDSC curves, which corresponds to a phase transformation that yields a thermotropic mesophase. The interplanar distance d of such a phase is 25.6607 Å and the long range cell parameter a should be equal 51.3216 Å. This agrees with the affirmation on the existence of one or more thermotropic phases in the form of liquid crystal for metallic carboxylates [19]. Also, this fact is in agreement with previous works which showed that the transition to a high temperature mesophase is accompanied by a conformational disorder within the chain [19].

3.4. Infrared spectroscopy with temperature

The evolution of the synthesized sample C_{11} with temperature was also followed by means of IR

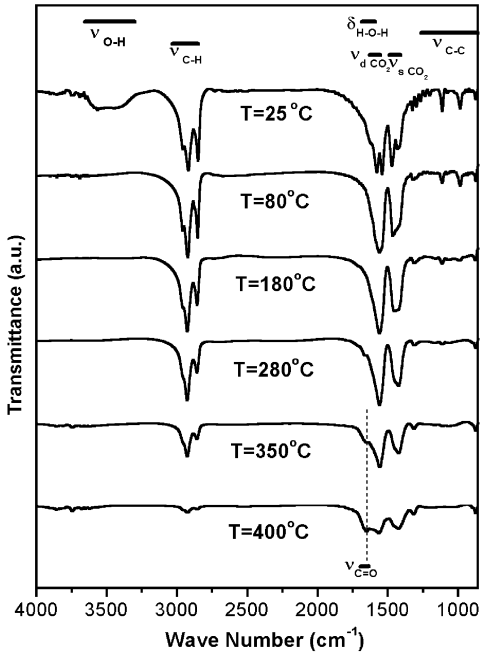

Fig. 8. Infrared spectra of C_{11}, measured at different temperatures. The absorption bands of interest have been indicated. The dashed line indicates the appearance of a C=O ketone band.

spectroscopy. In Fig. 8 the infrared spectra measured at several temperatures are shown. It can be seen that, for the used experimental conditions, the dehydration begins at 80°C. This is evident from the diminution of the stretching (ν_{O-H}) and bending (δ_{H-O-H}) absorption bands of water (indicated in Fig. 8).

On the other hand, the decomposition becomes evident around 180°C and begins indeed from the aliphatic chain, because the absorption bands that correspond to the stretching C–C vibrations disappear in the first place at this temperature. The breaking of C–C bonds of the chain would cause a reordering of hydrogen atoms in order to obtain the electrical charge balance, that would include the liberation of gaseous hydrogen. This can explain the occurrence of the mass loss effects observed in Hi-Res TGA curves at the beginning of the decomposition.

Nevertheless, it is necessary to indicate that our observations do not agree with the hypothesis which states that the decomposition passes through the formation of alkyl ($C_nH_{2n+1}^-$) and acyl (RCO^-) radicals, that soon react to form ketones without the necessity of the proton liberation to obtain the charge balance [21]. This difference could be given by the inequalities in the used experimental conditions, but a conclusive result could be only obtained making measurements of TGA together with a gas chromatography and/or mass spectrometry identification of the decomposition products.

The next stage in the decomposition is related to the C–H bonds breaking as it can be seen from the IR spectrum taken at 280°C, where the C–H stretching bands have diminished. Finally, at temperatures above 350°C the carboxylate group begins to be disturbed, which is reflected in a decrease of the intensity of the asymmetric and symmetric stretching bands of this group in the 1470–1420 cm^{-1} and 1610–1550 cm^{-1} regions (see Fig. 8). Next to this process a new absorption band appears, that has been indicated in Fig. 8 with a dashed line, and that can be assigned to the carbonyl group stretching vibrations in ketones. This is an indication of the ketone formation, which is in agreement with a previous work that affirms that the decomposition of aliphatic carboxylates gives rise to ketones [21].

3.5. Kinetic study. Model-free isoconversion method

Finally, the collected Hi-Res TGA data were processed using the isoconversion principle previously described [22] in order to obtain the dependency of the activation energy $(E_a)_\alpha$ as a function of the degree of transformation of the solid α. According to this principle the transformation rate $d\alpha/dt$ at constant extent of conversion, is only a function of temperature, and the function $f(\alpha)$, that describes the mechanism of the reaction, is independent of the heating rates. If the Arrhenius equation is applicable, we can write:

$$\left[\frac{d\ln(d\alpha/dt)}{dT^{-1}}\right]_\alpha = -\frac{E_\alpha}{R}, \quad (1)$$

where the subscript α indicates the values of isoconversion (equal degree of transformation) $(\alpha_i)_1 = (\alpha_i)_2 = \cdots(\alpha_i)_n$ for each one of the experiments $(1, 2, \ldots, n)$ and each temperature.

This criterion allows an estimation of $(E_a)_\alpha$ without the assumption of any reaction model, that is to say, it is a model-free method.

Figs. 9 and 10 show the obtained results when applying the "Eq. (1)" to a series of Hi-Res TGA experiments performed at different programmed heating rates for dehydration, as well as for the degradation stage of calcium undecanoate, respectively. This analysis showed, for all the evaluated thermal events, that the activation energy is independent on the degree of transformation α, under the experimental conditions used in this study.

The obtained average activation energy value of 157 ± 9 kJ/mol for the dehydration process (Fig. 9) in this salt is in agreement with values reported for other crystalline calcium hydrates [17].

The stage of decomposition (Figs. 6 and 10) shows three perfectly defined regions, however, its interpretation and assignment is difficult, because in this interval several simultaneous and complex processes can occur, these include, bonds rupture in C–C, CH_2 and CH_3 groups, melting, among others. All these considerations

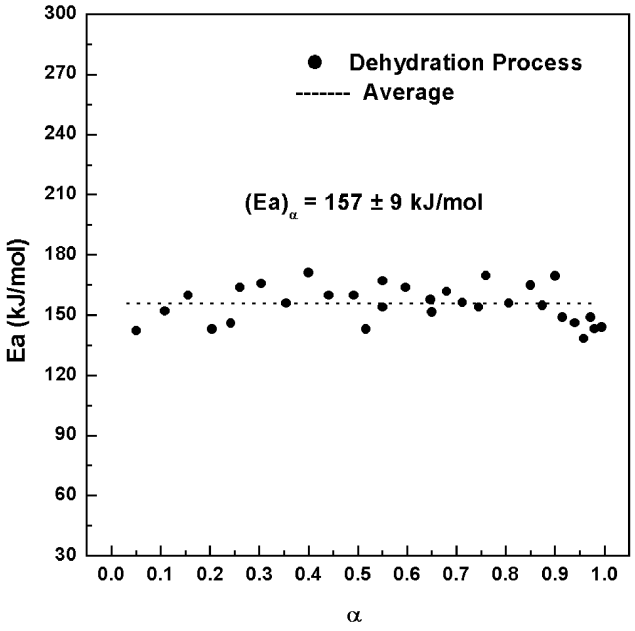

Fig. 9. Activation energy $(E_a)_\alpha$ as a function of the transformation degree α for dehydration of calcium undecanoate monohydrate.

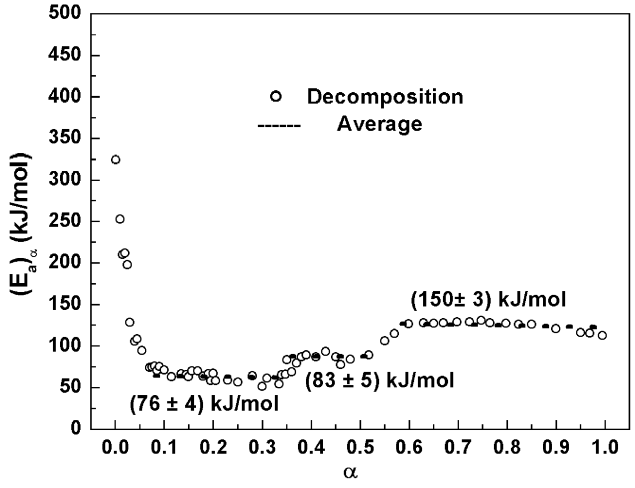

Fig. 10. Dependency of the activation energy $(E_a)_\alpha$ on the degree of conversion for calcium undecanoate decomposition process.

make difficult any kinetic study, because the possible evaluation of a triple kinetics in this temperature interval will have only a global or apparent character, without a clear physical meaning. A more detailed interpretation can be possible, as has been already noticed, through the identification of the gases of the decomposition, to identify the elementary step that limits the reaction in each one of these stages.

Nevertheless, the fact that the activation energy of these processes increases as the decomposition advances (Fig. 10) could be an evidence of the chain breaking. When the chain breaks it makes itself shorter and, in accordance with the calcium carboxylates behavior observed in our earlier work [5], where their thermal stability increases as the aliphatic chain length decreases, a higher activation energy would be needed to initiate any process as the chain becomes shorter.

Also it is possible to conclude from the results exposed in Fig. 10, that the reaction mechanism during these processes is unique, this means that the step that always limits the speed of the reaction is the same one, which does not exclude other simultaneous mechanisms of less importance. The validity of this criterion is confirmed by the fact that the activation energy, which is constant for each one of these processes, does not depend on the transformation degree (α).

4. Conclusions

The sample C_{11}, as synthesized from calcium hydroxide and undecanoic acid exists as calcium undecanoate monohydrate with the presence on a second minoritary phase that corresponds to the anhydrous calcium undecanoate.

The monohydrated phase showed to have monoclinic cell with cell parameters $a = 64.4473$ Å, $b = 6.8067$ Å, $c = 5.8892$ Å, $\beta = 90.70^\circ$ and a symmetry described by the $P2_1/a$ space group. This phase dehydrates at about 100°C, this process is accompanied by a phase transformation to a liquid crystalline phase. The reaction mechanism of the dehydration process is unique and does not depend on the heating rate. The activation energy value for dehydration is 157 kJ/mol.

The decomposition of calcium undecanoate happens in a wide range of temperatures, extending beyond 350°C. It occurs in several steps, starting from the aliphatic chain, with C–C bonds breaking, followed by C–H bonds rupture and finally by the carboxylate group decomposition.

At 300°C the salt melts and at 400°C the formation of ketones as decomposition products is observed.

Acknowledgments

The present research was partially performed at LNLS—National Synchrotron Light Laboratory, Brazil. A. Valor wants to thank LNLS for partial financial support for carrying out the project XRD858/01 and LNLS staff for their help and kindness. Also, the support with laboratory facilities of Dr. Ciro Falcony, as well as, the assistance of Eng. Marcela Guerrero and Eng. Angel Martínez are acknowledged.

References

[1] S.K. Upadhyaya, Indian J. Chem. 36A (1997) 1054–1057.

[2] E. Reguera, H. Yee-Madeira, J. Fernández-Bertrán, F. Sánchez-Sinencio, in: J.A. Heras, R.V. Jiménez (Eds.), Topics in Contemporary Physics, IPN, México, 2000, p. 22 (Printed by Monarch Litho INC. USA).
[3] A. Valor, Ph.D. Thesis, CICATA-IPN, México 2002.
[4] A. Valor, E. Reguera, F. Sánchez-Sinencio, Powder Diffraction 17/1 (2002) 13–18.
[5] A. Valor, E. Reguera, E. Torres, S. Mendoza, F. Sánchez-Sinencio, Thermochim. Acta 389/1–2 (2002) 133–139.
[6] P.M. de Wolf, J. Appl. Cryst. 1 (1968) 108–113.
[7] G.S. Smith, R.L. Snyder, J. Appl. Cryst. 12 (1979) 60–65.
[8] Stefan Krumm, WinFit, Ver. 1.2.1, 1997; available at http://www.geol.uni-erlagen.de.
[9] R. Shirley, The CRYSFIRE system for automatic powder indexing, 1999; available at http://www.ccp14.ac.uk.
[10] J. Laugier, B. Bochu, LMGP suite of programs for the interpretation of X-ray experiments, 2000; available at http://www.ccp14.ac.uk/tutorial/lmgp/.
[11] E. Torres-García, A. Peláiz-Barranco, C. Vázquez, F. Calderón Piñar, O. Pérez Martínez, Thermochim. Acta 39 (1–2) (2001) 372.
[12] E. Torres-García, A. Peláiz-Barranco, C. Vázquez-Ramos, G.A. Fuentes, J. Mater. Res. 16/8 (2001) 2209.
[13] K.N. Mehrotra, S.K. Upadhyaya, Recl. Trav. Chim. Pays-Bas 106 (1987) 625–627.
[14] A.J. Stosick, J. Chem. Phys. 18/8 (1950) 1035–1040.
[15] P. Lelann, J.-F. Bérar, Mater. Res. Bull. 28 (1993) 329–336.
[16] G. Reichmuth, E. Dubler, Thermochim. Acta 85 (1985) 485–488.
[17] D. Dollimore, W.E. Brown, A.K. Galway, in: Bamford and C.F. Tipper (Eds.), Comprehensive Chemical Kinetic, Elsevier, Amsterdam, 1980.
[18] C.A. O'Conell, D. Dollimore, Thermochim. Acta 357–358 (2000) 79–87.
[19] M.S. Akani, E.K. Okoh, H.D. Burrows, H.A. Ellis, Thermochim. Acta 208 (1992) 1–41.
[20] G.S. Hattiangdi, M.J. Vold, R.D. Vold, Ind. Eng. Chem. 41 (1949) 2320.
[21] R.A. Hites, K. Biemann, J. Am. Chem. Soc. 94 (16) (1972) 5772–5777.
[22] S. Vyazovkin, C.A. Wigth, Annu. Rev. Phys. Chem. 48 (1997) 125.